Evaluation of the Hydro Chemical Characteristics and Sources of Major Ions in Groundwater in Sheet 163 (Zungeru) North-Central Nigeria

¹Abdullahi, S. ²Garba, M.L. ¹Idris-Nda, A.

¹Department of Geology, Federal University of Technology, Minna.

² Department of Geology, Ahmadu Bello University, Zaria
E-mail: absuleiman@futminna.edu.ng

Abstract

This study presents a comprehensive hydrochemical analysis of groundwater in a specific area, focusing on major ions such as calcium (Ca²⁺), magnesium (Mg²⁺), sodium (Na⁺), potassium (K⁺), bicarbonate (HCO₃⁻), sulfate (SO₄²⁻), chloride (Cl⁻), nitrate (NO₃⁻), fluoride (F⁻), phosphate (PO₄), and ammonium (NH₄⁺). The concentrations of these ions were measured and analysed against Nigerian and World Health Organization (WHO) standards for drinking water quality. The findings reveal that the groundwater in the study area is generally within acceptable limits for drinking water quality, with concentrations of major ions falling within regulatory standards. The sources of these ions vary, with calcium and magnesium originating from calcium-rich rocks and metasediments, while sodium is derived from clays and minerals like feldspars. Potassium may stem from K-bearing minerals or agricultural practices. Bicarbonate exhibits the highest concentration among the analysed ions, indicating its prevalence in the groundwater. Sulfate concentrations are below recommended limits, possibly originating from the dissolution of minerals in amphibolites. Chloride levels, though within permissible limits, show localized increases around areas with anthropogenic activities like waste disposal. Nitrate concentrations indicate potential pollution sources, including decaying organic matter and agricultural practices. Fluoride levels are generally below maximum limits, with possible sources being fertilizer and agrochemical leaching. Phosphate concentrations, primarily from agricultural activities, remain within acceptable ranges, except for a few samples. Physical parameters such as pH, total dissolved solids (TDS), and electrical conductivity (EC) provide further insights into groundwater quality. The dominance of calcium and bicarbonate ions reflects geological influences, while elevated nitrate and chloride levels suggest anthropogenic contributions. Hydrogeochemical analyses, including Piper trilinear plots, Durov plots, and Stiff diagrams, elucidate groundwater facies and geochemical processes. Seasonal variations in water types and geochemical evolution are observed, with different water facies identified during wet and dry seasons. The study underscores the importance of comprehensive hydrochemical analyses in understanding groundwater quality, identifying potential pollution sources, and informing sustainable water resource management strategies in the study area. Further research could explore long-term trends and dynamic interactions between hydrogeochemical processes and anthropogenic activities.

Keywords: Anthropogenic sources; Environmental contamination; Groundwater quality; Hydrogeological characteristics; Water facies

INTRODUCTION

Groundwater, as a vital component of the hydrological cycle, plays a pivotal role in sustaining ecosystems and human activities worldwide (Acharya & Barbier, 2000; Zacchaeus et al., 2020). Understanding its chemical composition and the sources of major ions is crucial for managing water resources effectively, ensuring water and mitigating potential quality, environmental risks (Ige et al., 2021). Hydrochemical analysis provides valuable insights into the characteristics groundwater, shedding light its geochemical evolution and the processes influencing its composition (Siloko et al., 2022).

In the of study groundwater hydrochemistry, major ions such as calcium (Ca²⁺), magnesium (Mg²⁺), sodium (Na⁺), potassium (K⁺), bicarbonate (HCO₃⁻), sulfate (SO₄²⁻), chloride (Cl⁻), nitrate (NO₃⁻), fluoride (F-), phosphate (PO₄-), and ammonium (NH₄⁺) are key indicators used to assess water quality and identify potential sources of contamination. The concentrations of these ions can vary significantly based geological on formations, hydrological conditions, anthropogenic activities, and climatic factors.

Calcium, a common cation in groundwater, often originates from the weathering of calcium-rich rocks such as limestone and gypsum (Lawal et al., 2022). Magnesium, another prevalent cation, is derived from the dissolution of magnesium-bearing minerals present in various geological formations (Ige et al., 2021). Sodium and potassium ions are often associated with the weathering of silicate minerals and can also enter groundwater through anthropogenic

sources such as agricultural practices and wastewater discharge (Sikakwe & Eyong, 2022). Bicarbonate, sulphate, chloride, nitrate, fluoride, phosphate, and ammonium ions are important anions found in groundwater, each with distinct sources and implications for water quality. Bicarbonate ions, for example, are often produced through the weathering of carbonate minerals and play a crucial role in buffering the pH of groundwater (Akinfemiwa & Kofoworola, 2023). Sulphate and chloride ions can originate from natural processes such as the oxidation of sulphide minerals and the weathering of rock formations, as well as from anthropogenic sources like industrial activities and urban runoff (Long et al., 2021). Nitrate contamination in groundwater is frequently linked agricultural activities, sewage discharge, and the use of nitrogen-based fertilizers (Wu et al., 2021). Fluoride concentrations in groundwater can vary depending on the underlying geology, with elevated levels posing health risks to human populations (Onipe et al., 2020). Phosphate and ammonium ions, primarily derived from agricultural runoff and domestic sewage, can contribute to eutrophication and ecosystem degradation in groundwater systems (Wurtsbaugh et al., 2019).

In addition to hydrochemical analysis, understanding the spatial distribution and hydrogeological characteristics of groundwater is essential for comprehensive water resource management. Factors such as geological formations, aquifer properties, groundwater flow patterns, and recharge dynamics influence the transport and fate of major ions in groundwater systems.

The rock types encountered in the mapped area include migmatite-gneisses, schists,

amphibolites, quartzites and minor granitic intrusions as shown on the geological map. The gneisses occupy most of the study area and include the granite gneiss and the banded gneiss. Both gneisses and the schist were intruded by the granites. The gneisses occur as hilly, massive, and low-lying outcrops, where they form contact with the schists around Ushama, Gelenge, Garin Gabas and Yakila villages. The schist and amphibolites occupy the central part of the study area and are bounded approximately N-S trending units of the migmatites-gneiss complex around Zungeru. The contact with the gneisses may be tectonic in places and is marked by development of cataclastics and mylonites around the Kaduna River at Zungeru (Agbor, 2014). The amphibolites occur in association with quartzites and association suggests that both rocks must have been deposited by sediments and later metamorphosed to form amphibolites and quartzites (Turner, 1983). Shortly after Kundu village, there are two sub-parallel quartzite ridges approximately fifty (metres apart) with a strike length of over two kilometres (2km) east of the tarred road. These quartzite ridges are 20m in width each and terminated 1km before Garun Gabas village (N09° 52' 25", E06° 07' 21 and N09° 52' 28", E06° 07' 37"). Within the study area, two varieties of amphibolites were encountered. They are the dark green and foliated variety found around Zungeru, Kamfanin Kirya and Kodo villages and greenish and massive varieties are found around Maikunke. The banded varieties are medium grained, strongly foliated, and dark green in colour whereas the massive variety is fine to medium grained, weakly foliated and dark grey in colour.

Agbor, (2014) reported large bodies of amphibolite within the study area and described the contact between amphibolites and the quartzo-feldsparthic rocks as sharp in some areas while in others transitional. the contacts are The transitional contacts mapped by Elueze, et al., (2003) made him to conclude that the amphibolites were probably derived from calcareous sediments.

Granitic rocks were mapped around Kunu Manta Beri and Outskirt of Maikunkele village. These outcrops trends in the NW-SE direction (N315⁰E). The rocks are massive and coarse textured with few fractures displayed in some places.

This study aims qualitatively to characterize and assess the vulnerability of groundwater to pollution in Sheet 163 (Zungeru), North Central Nigeria. The objectives include conducting geological and hydrogeological mapping, determining chemical characteristics of groundwater, evaluating the impact of trace elements on agricultural, domestic, and mining activities, comparing analysis results with reference values for human health and environmental impact assessment, and producing vulnerability maps and models for the study area. The research scope covers the Kushaka schist belt of North Central Nigeria, employing field mapping, static water level measurements, pump test data collection, water sample analysis, and in-situ determination of physical parameters.

Study Location and Geology

The area of study is located within Niger state and covers Sheet 163 (Zungeru). It is bounded within latitudes 09° 30′ N and

10°00′ N and longitudes 6° 00′ E and 6° 30′ E (Figure 1).

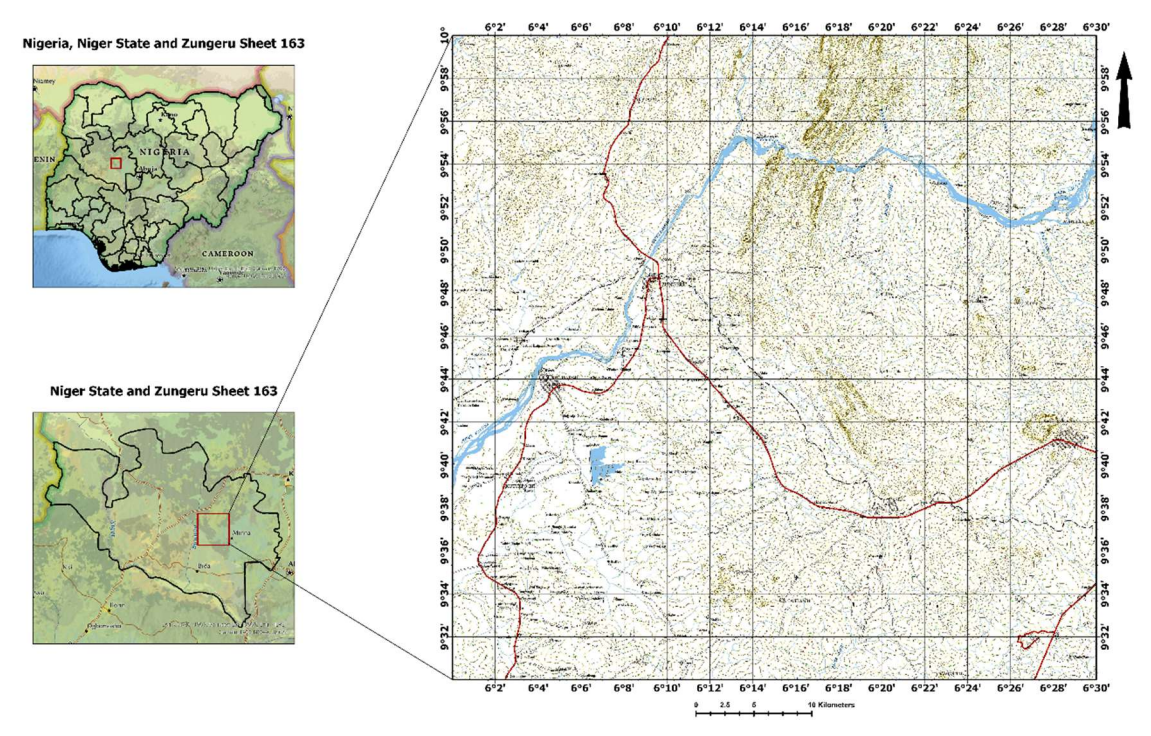


Figure 1: Location map of the study area.

Nigerian Basement Complex crystalline rocks underlie the research area. The study area includes Katako and Yakila in the north, Kutunku in the north-west, Maikunkele in the northeast, and Tangwagi in the south. Good roads connect it to the rest of the country. North of Tegina, Wushishi and Bida to the southwest, and Minna to the southeast are key roadways. Accessible via numerous local roads, footpaths, and the Zungeru-Minna-Kano and Zungeru-Lagos rail lines from the North and South, respectively.

Zungeru is a valley town surrounded by highlands that shape the watershed for its river systems. Local rivers include the Kaduna, Innamayi, and Tausheta. Therefore, nearby towns and villages are higher. Many seasonal rivers and streams drain the study region, flowing during the rainy season and dry during the dry season. The study region

is well-drained due to its dendritic drainage structure and several stream systems.

environment has tropical high temperatures (31.2°C–36.9°C), clear skies, and wet and dry seasons (https://www.nimet.gov.ng/seasonalclimate-prediction). The dry season lasts from November to April with low humidity and North-East trade winds during harmattan. From 40% in early March to 94% in September, relative humidity rises. Wet season runs from April to November (https://www.nimet.gov.ng/seasonalclimate-prediction). The average monthly rainfall is about 300 mm in September. In the Guinea Savannah belt, plants and forests grow along water channels.

The study location is in northwestern Nigeria's Kushaka schist Belt (Figure 2). Low-grade, metasediment-dominated

Schist Belts going N–S are best developed in western Nigeria. Upper Proterozoic supracrustal rocks infolded into the migmatite-gneiss-quartzite complex form these belts. Schist belts have coarse to fine-grained clastics pelitic schists, phyllites, banded iron formation, carbonate rocks (marbles), and mafic metavolcanics. Some contain ocean floor pieces from minor back-arc basins. Rahaman (1976) and Woakes et al. (1987) indicate various deposition basins, while Oyawoye (1972) and McCurry (1976) view the schist belts as relics of a single supracrustal cover.

Olade and Elueze (1979) call Schist belts fault-controlled rifts. Turner (1983)suggests sediment ages based on structural and lithological correlations. Ajibade et al. (1979) disagreed and proved that both series had identical deformational histories. Truswell and Cope (1963) considered the belt-basement schist structural relationships conformable metamorphic fronts, while Ajibade et al. (1979) first mapped the structural break.

Geochronology of schist belts is challenging, however Ogezi (1977)accepted a metamorphic age of $1,040 \pm 25$ Ma for the Maru Belt phyllites based on the intrusive cross-cutting Older Granites. Most Schist Belt rocks are Upper Proterozoic. The geochemistry of schist belt amphibolite complexes is likewise controversial. Klemm et al. (1984) suggest the Ilesha belt is Archaean greenstone. Olade and Elueze (1979), Ogezi (1977), and Ajibade (1980) support ensialic processes in schist belt evolution, while Woakes et al. (1987) and Egbuniwe (1985) emphasise marine materials with tholeiitic affinities. Some metallogenetic features of the schist belts may be relevant to these

problems: the apparent of absence subduction-related mineral deposits may indicate a limited role for ensimatic processes; the distribution of primary gold occurrences in some belts but its marked absence in others may indicate that they do not represent single supracrustal Schist belts are most developed in western Nigeria, west of 8° E longitude, with isolated occurrences in the east. The belts are limited to a 300-km NNE trending zone. Burke and Dewey (1972) Dahomeyan gneisses and migmatites lie west of this zone. To the east, no schist belts are recorded for 700 km until Cameroun, where Upper Proterozoic belts occur in Pan-African granite-migmatite terrain north of the Congo Craton. Schist Belts linked with gold mineralization have been extensively plotted and researched in Maru, Anka, Zuru, Kazaure, Kusheriki, Zungeru, Kushaka, Isheyin, Oyan, Iwo, and Ilesha.

According to the 2013 version of the Nigeria Geological Survey Agency (NGSA) geological map of Niger State, Rafi and its environs are predominantly underlain by migmatitic rocks of tectonic origin that have suffered from high grade regional metamorphism. The migmatites are in contact with a unit of amphibolite schist/amphibolite to the north-central and a unit of phyllite and quartzite schists interlayered with amphibolite to southwest of the area. Large scale intrusions of medium to coarse grained biotite granite and undifferentiated units of porphyritic granites/coarse porphyritic biotite and biotite hornblende granites are also outcropped within the migmatite resulting to localised steep dips in the area. A NNE-SSW anticlinal structure is also shown by the NGSA map resulting from the

high deformational history suffered by the rocks.

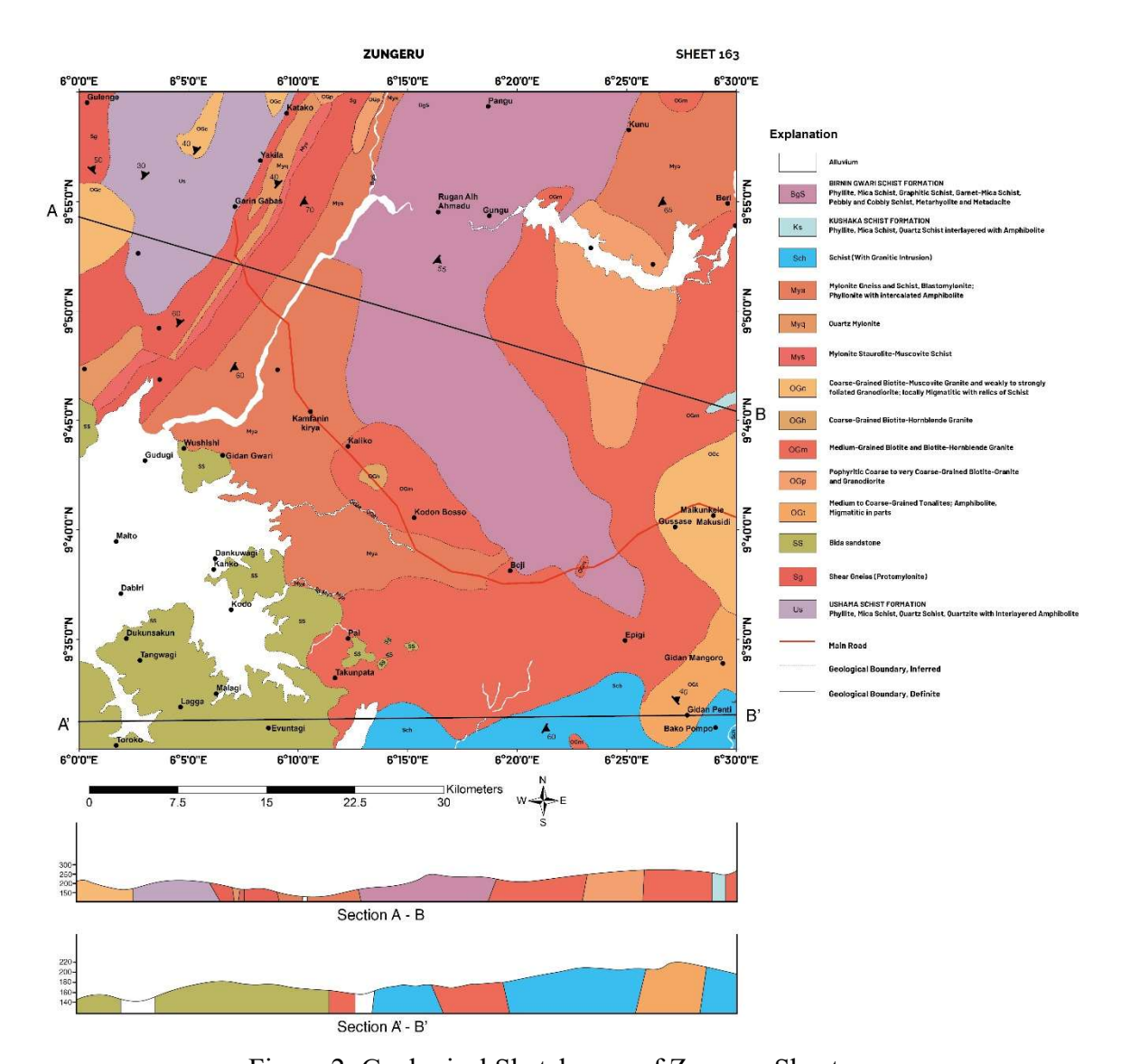


Figure 2: Geological Sketch map of Zungeru Sheet

MATERIALS AND METHODS

Data Collection

In the developing world groundwater is generally preferred as a source of potable water this is because it is readily available and naturally protected from contamination. According to Golchin, and Azhdar (2016), groundwater chemistry could reveal important information about the geological

history of the aquifers and the suitability of groundwater for domestic, industrial, and agricultural purposes. The chemistry of groundwater is largely control by its mineral composition and formation through which water flows (Elango and Kannan.,2007). In order to characterize the groundwater in this terrain, groundwater samples were collected from forty-five (45) open water wells for both wet and dry

These water samples were seasons. analyzed for major and trace elements using different analytical techniques to evaluate the hydro-geochemistry of the groundwater obtained from the different aquifers. The major Cations analyzed are Calcium, Magnesium, Potassium and Sodium while the anions analyzed includes Sulphates, Bicarbonates and Chlorides. The other ions analyzed includes Ammonium, Nitrites, Fluorides and Phosphates. Trace or heavy metals were also analyzed for in the groundwater samples these were Total iron, Chromium, Cadmium, Manganese, Copper, and Zinc.

To prepare the collected samples for analysis, a meticulous filtration process will be employed. Using a 0.45-micron filter will effectively remove suspended particles and other unwanted debris, guaranteeing the purity and accuracy of the samples that will be analysed later. This rigorous methodology underscores the commitment to maintaining the quality and reliability of the data acquired, thereby enhancing the robustness of the research findings, and contributing to the advancement of geoscientific understanding in the fields of hydrology and water resource management.

Water Samples Analysis

The determination of cations, including Na, K, Ca, and Mg, will be conducted employing either Atomic Absorption Spectroscopy (AAS) or Inductively Coupled Plasma Mass Spectrometry (ICP-MS) techniques. These analytical methods offer high precision and sensitivity in detecting trace elements within the samples. The concentration of each cation (C_{cat}) will be quantified utilizing the formula:

$$C_{cat} = \frac{A_{sample}}{A_{standard}} \times C_{standard}$$

1

where A_{sample} represents the absorbance of the sample, $A_{standard}$ denotes the absorbance of the standard solution, and $C_{standard}$ signifies the concentration of the standard solution.

The rigorous determination of anions, encompassing Cl, SO₄, CO₃, HCO₃, F, and NO₃, will be achieved through ion chromatography, a specialized technique tailored for the precise analysis of ionic species within aqueous solutions. The concentration calculations for anions will be contingent upon the specific methodology employed during chromatography, accounting for factors such as retention times, peak areas, and calibration curves established through standard reference materials.

The determination of metals, including Fe, Al, Ba, Cu, Ni, As, Hg, Co, Pb, Mn, and Cr, will be conducted utilizing state-of-the-art techniques such as Inductively Coupled Plasma Mass Spectrometry (ICP-MS) or Inductively Coupled Plasma Optical Emission Spectrometry (ICP-OES).

The concentration of each metal (C_{met}) will be computed using the formula:

$$C_{met} = \frac{A_{sample}}{A_{standard}} \times C_{standard}$$

2

where A_{sample} represents the absorbance of the sample, $A_{standard}$ denotes the absorbance of the standard solution, and $C_{standard}$ signifies the concentration of the standard solution.

This rigorous analytical approach ensures accurate and reliable quantification of metal concentrations, providing valuable insights into the environmental and geochemical characteristics of the sample matrix. In parallel, the determination of non-metal parameters, specifically NH₄ and PO₄, will be executed through either spectrophotometric methods or colorimetric analysis. These techniques leverage the distinctive absorption or colour properties exhibited by these compounds to facilitate their quantitative assessment.

Concentration calculations for NH₄ and PO₄ will be predicated on calibration curves derived from standard solutions of known concentrations. Bvcorrelating absorbance or colour intensity of the with the corresponding sample concentration values obtained from the calibration curve, the precise concentrations of NH₄ and PO₄ can be accurately determined.

The methodologies employed for physicochemical analysis in this study have previously been utilized in other geochemical investigations, as demonstrated in Adetunde et al. (2011).

(a) Physical Parameters Certified international standard methods were employed to determine these parameters.

Total Dissolved Solids (TDS) (APHA, 1998): TDS were directly measured using a TDS meter.

(b) Chemical Parameters Various techniques were employed to analyse the chemical parameters in the laboratory, including methods outlined by (APHA, 1998) and (WHO, 2006). These methods encompassed:

- (i) Volumetric titration method (WHO, 2006): Chemicals were subjected to titration with a standardized titrant, and the endpoint was indicated by a colour change using an indicator.
- (ii) Colorimetric method (WHO, 2006): The intensity of colour from target chemicals was measured, and the measured potential was logarithmically proportional to ion concentration.
- (iii) UV Method (WHO, 2006): Similar to the colorimetric approach, this method utilized UV light to measure the absorption of certain organic compounds, revealing a correlation between UV absorption and organic carbon content for qualitative estimation.
- (iv) Atomic Absorption Spectrophotometry (AAS) Method (WHO, 2006): This technique was employed for identifying metal elements.

The following chemical parameters were assessed in this study: a. Alkalinity was determined through titration using methyl orange as an indicator. b. Total hardness and calcium ion concentration were assessed via titration using standard EDTA at pH 10, with Eriochrome black T as an indicator. c. Chloride content was calculated using argentometric an procedure, involving titration with standard silver nitrate and the indicator potassium chloride. d. Iron, manganese, and lead ion content were measured using Unicam 969 Atomic Absorption Spectrophotometry (AAS). e. Sulphate ion levels were determined using a colorimetric procedure (APHA, 1998).

The concentrations of the major constituent cations and anions were converted from

milligram/litre (mg/L) to milliequivalent/litre (meq/L) and Percentage equivalent mass (% epm) using the equation 3.1 developed by Todd (1980)

 $Mean equivalent mass = \frac{Atomic weight}{Valency}$

3

$$\frac{\text{Concentrations}\left(\frac{\text{meq}}{\text{L}}\right) = \\ \frac{\text{Concentrations}\left(\text{mg/l}\right)}{\text{Equivalent mass}}$$

4

% epm =
$$\frac{\text{Concentrations (meq/l)}}{\text{Total Cation or Anion}} \times 100$$

5

The concentrations in meq/L were used to prepare Piper trilinear, Schoeller Semi logarithmic, Durov and Stiff diagrams.

The total hardness as (CaCO₃) of the borehole water samples in study area were determined using equation 3.4 developed by Todd (1980). Total hardness as

$$CaCO_3 mg/L = 2.5 [Ca^{2+}] + 4.1 [Mg^{2+}]$$

6

Water Quality Index (WQI)

WQI was computed by making use of the weighted arithmetic index formula. The quality rating scale (q_i) for each parameter was obtained by dividing the sample concentration (C_i) in each groundwater sample by its respective standard (S_i). The result is then multiplied by 100 (Akakuru & Akudinobi 2018; Gopinath et al., 2019).

$$WQI = \frac{\sum W_n Q_n}{\sum W_n}$$

7

Where W_n is the unit factor for each parameter used in the calculation and is gotten by

$$W_n = \frac{K}{S_n}$$

8

$$K = \frac{1}{\frac{1}{S_1 + \frac{1}{S_2} + \frac{1}{S_3 + \dots + \frac{1}{S_n}}}} = \frac{1}{\sum \frac{1}{S_n}}$$

9

 $S_n = Standard Limit of the nth parameter$

On summation of all the selected parameter unit weight factors, $W_n = 1$ (unity)

Q_n is the sub-index

$$Q_n = \frac{[(V_n - V_0)]}{[(S_n - V_0)]} \times 100$$

10

Were,

Vn =mean concentration of the nth parameter

 $S_n = Standard Limit of the nth parameter$

 V_0 = Actual value of the parameter in pure water (V0=0, for most parameters except for pH

Table 1: Water Quality Index Classification and Status (According to Brown et al., 1972)

WQI Classification Index	Water Quality Status
0-25	Excellent
26-50	Good
51-75	Poor
76-100	Very Poor
>100	Unfit for Consumption

Hydrogeochemical Plots

In this study, a relatively extensive dataset was employed to assess these techniques and to compare their effectiveness in sorting water chemistry samples into coherent groups. Specifically, the techniques of Stiff diagram, Piper diagram, Schoeller diagram, and Durov diagram were selected for this research.

Graphical techniques often focus on specific components or subclasses of the available data, whereas statistical methods can handle the entirety of the given data. The main objective of comparing these techniques is to identify the chemical similarities among water samples. Samples exhibiting similar chemical patterns often share comparable hydrologic histories, including factors like recharge areas, mineral composition, infiltration routes, flow pathways in relation to climate, and time.

Piper diagram

This refers to a graphical representation of water chemistry, depicting both positive and negative ions using distinct ternary plots. The cation plot highlights calcium,

magnesium, sodium, and potassium peaks, while the anion plot showcases sulfate, chloride, carbonate, and bicarbonate peaks. These two ternary plots are projected onto a diamond shape, serving as a condensed matrix representation of both anions and cations within a graph. Unlike the Stiff diagram, concentrations in the Piper diagram are expressed in terms of % meg/L. Numerous test results can be plotted on the same diagram, making it valuable for classifying waters based on hydrochemical facies. The Piper diagram is particularly useful for identifying water mixing and tracking changes across space and time. Nonetheless. its concentrations renormalized, and it may not readily accommodate other relevant cations or anions that should not be disregarded.

Durov diagram

The Durov diagram in AquaChem which is an alternative to the Piper diagram. The Durov diagram shows the major ions as percentages. The total cations and the total anions are set equal to 100% and the data points in the two triangles are projected onto a square grid that lies perpendicular to the third axis in each triangle. The plot establishes useful properties for large

sample groups. The benefit of the Durov diagram is to elaborate clustering of data points to point out samples that have similar compositions. The Durov diagram can be used to plot either selected sample groups or all samples in a data set.

Stiff Diagram

A Stiff diagram is a graphical representation of water chemistry that plots the concentrations of major ions, such as Ca, Mg, Na, K, Cl, SO4, and HCO3, on a single diagram. It helps visualize the relative proportions of different ions in water samples and can indicate the dominant geochemical processes influencing water chemistry, such as weathering, evaporation, or ion exchange.

Gibbs Plot

The Gibbs plot relates the ratios of major ions in water samples to the ionic strength of the water. It helps identify the dominant hydrogeochemical processes controlling water chemistry, such as rock weathering, evaporation, or precipitation, based on the position of data points relative to theoretical curves on the plot.

Schoeller Diagram

The Schoeller diagram is used to assess the origin and evolution of groundwater by plotting the isotopic compositions of hydrogen and oxygen (δ 2H and δ 18O) against each other. It helps identify sources of groundwater recharge, mixing processes, and evaporation effects, aiding in the

understanding of groundwater flow dynamics and recharge mechanisms.

RESULTS AND DISCUSSION

The results from groundwater analysis for seasons one and two, as summarized in Tables 2 and 3 respectively, provide valuable insights into the hydrochemical characteristics and variations over time.

In season one, the analysis reveals a wide range of concentrations for key ions such as sodium (Na), potassium (K), calcium (Ca), and chloride (Cl). Sodium levels range from 2.000 to 260.000 mg/L, indicating significant variability in groundwater composition. The mean chloride concentration is 15.153 mg/L, with a maximum value reaching 65.000 mg/L, suggesting potential sources contamination. Bicarbonate (HCO₃) levels exhibit considerable variability, ranging from 16.000 to 158.000 mg/L.

Season two analysis shows distinct patterns compared to season one, with notable changes in the concentrations of several key parameters. Calcium concentrations range from 10.090 to 121.950 mg/L, indicating variability in groundwater mineralization. Iron (Fe) concentrations range from 1.130 to 2.790 mg/L, highlighting potential influences from geological formations and anthropogenic activities. Chloride levels vary from 15.580 to 58.150 mg/L, suggesting fluctuations seasonal in groundwater quality.

Table 2: Descriptive Statistical summary of groundwater analysis for season one

	Minimum	Maximum	Mean	Std. Deviation	Variance	
Na	2.000	260.000	49.911	54.454	2965.219	
K	0.000	33.280	8.173 9.447		89.238	
Ca	0.590	330.320	47.466	54.601	2981.315	
Mg	0.100	19.470	7.592	5.247	27.530	
Fe	0.000	1.660	0.191	0.355	0.126	
Al	0.000	4.330	0.420	0.905	0.819	
Ba	0.000	0.780	0.178	0.161	0.026	
Cu	0.000	0.020	0.005	0.004	0.000	
Ni	0.000	0.030	0.004	0.005	0.000	
As	0.000	1.560	0.495	0.482	0.232	
Hg	0.000	0.080	0.031	0.019	0.000	
Co	0.010	0.030	0.018	0.005	0.000	
Pb	0.010	0.050	0.017	0.007	0.000	
Mn	0.000	2.360	0.081	0.352	0.124	
Cr	0.000	0.010	0.000	0.001	0.000	
C1	0.000	65.000	15.153	16.628	276.482	
SO_4	0.000	89.000	15.663	21.083	444.512	
CO_3	0.000	1.300	0.109	0.263	0.069	
HCO_3	16.000	158.000	70.200	28.678	822.436	
F	0.000	0.920	0.085	0.177	0.031	
NO_3	0.000	107.070	6.892	17.476	305.403	
NH_4	0.200	4.200	1.627	0.980	0.960	
PO_4	0.000	5.740	0.518	1.359	1.847	

A comparison between the two seasons reveals temporal variations in groundwater chemistry, likely influenced by factors such as hydrological conditions, land use changes, and anthropogenic activities. Seasonal fluctuations in key parameters

such as chloride, bicarbonate, and calcium underscore the dynamic nature of groundwater systems and the need for continued monitoring and management efforts.

Hydrochemical Analysis and Sources of Major Ions in Groundwater

Calcium Ca²⁺

The concentration of detectable calcium in the groundwater of the study area ranged between 0.59 and 330.32 mg/L with an average value of 47.46 mg/L, with all concentrations of Ca²⁺ falling within the

Nigerian standard for drinking water quality (NSDWQ) and the World health organization (WHO) acceptable limits.

The probable source of the high concentrations of calcium in some of the analyzed water samples could be from the dissolution of calcium rich rocks like pegmatites and from the sedimentary rocks and at the transition zones around Wushishi

and Maito. However, lower Ca²⁺ ion concentrations were recorded from the water samples that were collected from the

western and South western parts of the study area were the geology of the area were predominantly sedimentary in nature.

Table 3: Descriptive Statistical Summary of groundwater sample analysis for Season Two

	Minimum	Maximum	Mean	Std. Deviation	Variance
Na	0.010	9.030	4.928	2.140	4.581
K	0.190	12.680	5.979	3.014	9.083
Ca	10.090	121.950	32.086	19.277	371.593
Mg	0.120	32.400	17.149	8.203	67.288
Fe	1.130	2.790	1.351	0.357	0.128
Al	0.120	4.460	0.558	0.906	0.820
Ba	0.020	0.830	0.228	0.166	0.028
Cu	0.000	1.630	0.177	0.301	0.091
Ni	0.000	0.230	0.093	0.062	0.004
As	0.005	0.026	0.013	0.005	0.000
Hg	0.005	0.026	0.013	0.005	0.000
Co	0.012	1565.000	0.404	0.481	0.232
Pb	0.040	0.130	0.054	0.022	0.000
Mn	0.005	2444.000	0.102	0.361	0.130
Cr	0.000	1.380	0.231	0.389	0.151
Cl	15.580	58.150	31.290	10.400	108.159
SO_4	4.650	16.950	7.873	2.871	8.244
CO_3	0.000	0.000	0.000	0.000	0.000
HCO_3	2.580	65.450	18.843	11.068	122.509
F	0.000	0.915	0.083	0.177	0.031
NO_3	0.350	6.620	2.325	1.675	2.807
NH_4	0.070	6.570	2.223	1.690	2.856
PO_4	0.140	1.260	0.458	0.322	0.104

Magnesium (Mg²⁺)

The concentration of magnesium in the sampled groundwater of the study area ranged between 0.10 and 19.47 mg/L with an average of 17.15mg/L. The sources of magnesium in the groundwater from the could be study area from Metasediments (Amphibolites and Schist). All measured magnesium concentrations were within the Nigerian standard for drinking water quality (NSDWQ) and the World health organization (WHO) acceptable limits.

Sodium (Na⁺)

Sodium ion concentration varies between 2.0 mg/L with an average of 260 mg/L. The sources of Na+ in the analyzed groundwater samples are clays and minerals like feldspars, all the sodium concentrations of the study area were within the accepted limits of the WHO and NSDWQ except for two samples (Kundu and Beri). The possible source of the high concentration of Na+ in these water samples could be as a result of pollution by sewage effluents.

Potassium (K⁺)

The mean value of potassium in the groundwater of the study area is 8.17 mg/L with concentration that range between 0.00 and 33.28 mg/L. Potassium (K⁺) in the groundwater of the area are derived as a product of K-bearing minerals like clay minerals or from Agricultural fertilizers and house and animal waste manure applied on cultivated farmlands. The concentration of K+ in the water is within the accepted limits of the Nigerian and World health organization standards.

Bicarbonate (HCO₃-)

Bicarbonate ion has the highest concentration in the groundwater of the study area when compared to any other analyzed ion detected in this study. The concentration of HCO₃⁻ in groundwater range between 16 and 158 mg/L with an average value of 70.20 mg/L

Sulphate (SO₄ ²⁺)

Sulphate ion concentration in the area were far below the set recommended limits of both NSDWQ (2015) and WHO (2017) of 100 and 400 mg/L, respectively. The average concentration of sulphate of in the groundwater of the study area is 13.63 mg/L, while the concentration ranges between 0 and 28.29 mg/L. Possible origin of SO₄ ²⁺ in the groundwater is from the dissolution of minerals in amphibolites associated with rocks of Ushama shist.

Chloride (Cl⁻)

The chloride concentration of groundwater in the area of study range between 15.58 and 58.15 mg/L while the average concentration of Cl⁻ in the area studied was

31.29 mg/L. The highest Cl concentration values were recorded around Epigi area. The most likely sources of this ion in groundwater of the study area were probably from anthropogenic sources that includes the leached refuse dump, human and animal waste used as manure that percolated into the shallow groundwater body. All recorded concentrations fall within maximum permissible limit of 250 mg/L of both NSDWQ and WHO.

Nitrate (NO₃-)

Nitrate concentration in the area ranges between 0.35 and 6.62 mg/L while the average is 2.3 mg/L. The sources of NO₃-in the groundwater of the area includes both natural and anthropogenic sources however, the presence of elevated nitrate in groundwater of the area of study is an indication of pollution which includes decaying organic matter, human and animal waste as well as agrochemicals and fertilizer application.

Fluorite (F⁻)

Out of the 45 well water sampled and analyzed for fluoride only four samples had Fluoride in them with the concentrations ranging from 0.00 mh/l to 0.9 mg/l. These values fall below the 1.5 mg/L maximum permissible limits of the NSDWQ and WHO. However, majority of the sampled groundwater had fluoride values that were less than 0.5mg/L. Sources of the Fluoride in groundwater detected could be due to the leaching of fertilizer and agrochemicals applied in the irrigated area of these floodplain in the shallow groundwater. Natural sources of fluoride in the water can possibly be from rocks that are rich in micas and illites (clay fractions) which contain appreciable quantity of the mineral Fluorites.

Phosphate (PO₄-)

The principal possible sources of Phosphate in groundwater of the study area is basically anthropogenic due to the use of phosphate agricultural fertilizers, animal leaking septic systems or domestic wastewater. Phosphate concentration in the area of study ranges between 0.14 and 1.26 mg/L with an average of 0.45 mg/L. The concentration of PO₄ in groundwater is below the 2.5 mg/L of the U. SEPA. However, nine out of the 45 samples contain phosphate. The wells had PO₄concentration that ranges between 2.98 and 4.34 mg/L, this high concentration may indicate possible anthropogenic sources mostly arising from agricultural practices that includes Fertilizer application and other agrochemicals on irrigated farm lands.

Ammonium (NH4⁺)

Ammonium concentration of groundwater in this study ranged between 0.07 and 6.57 mg/L while the average was 2.22 mg/L. Sources of the NH₄⁺ in groundwater could be from decaying organic matter in soil or from leached fertilizer and other agrochemical applied on cultivated farms.

All the water samples collected had ammonia below both the WHO and NSDWQ standards for drinking water quality.

Physical Parameters of Sampled Groundwater

Table 4 provides information on the geographic coordinates (longitude and latitude) and the predominant rock types present at each sampling location, including Granite, Schist. **Biotite** Granite. Amphibolite, Sandstone. The and document also specifies the elevation (in metres) and well depth, which are crucial elements affecting groundwater flow patterns and recharge dynamics. Table 4 includes a range of physical parameters such as pH, temperature (in degrees Celsius), electrical conductivity (EC in uS), and total dissolved solids (TDS in mg/L), providing information on water quality and its appropriateness for different uses. The variety in physical parameters between the sampling sites highlights the different hydrogeological conditions and anthropogenic influences present in the research area. Analysing physical different parameters in geological formations and locations can help identify variations in groundwater quality and probable sources of contamination.

Table 4: Results physical parameters from the water samples

ID	Locations	Long	Lat	Rock type	Elevation (m)	well depth	pН	TEMP (0c	EC (Us)	TDS mg/l
ZNG	Gidan Mangoro	6.49	9.565	Granite	222	3.0	5.89	29.8	99.5	59.7
101										
ZNG	Gidan Penti	6.462778	9.525556	Granite	226	3.7	6.55	29.7	337.0	205
102 ZNG	Bako Pompo	6.484444	9.516111	Schist	198	3.6	6.74	32.0	549.0	331
103	Вако Гопіро	0.404444	9.510111	Schist	190	3.0	0.74	32.0	349.0	331
ZNG	Maikunkele	6.482778	9.6775	Biotite Granite	276	3.4	6.21	32.3	130.7	77.9
104										
ZNG	Beji	6.328056	9.635556	Biotite Granite	265	7.6	5.81	32.0	163.3	100
105		C 453 C11	0.660000	D: :: C ::	260	7 .0	6.24	22.6	260.0	161.6
ZNG 106	Gussase	6.453611	9.668889	Biotite Granite	269	5.8	6.34	33.6	269.0	161.6
ZNG	Tsohon	6.176111	9.756667	Amphibolite	146	7.2	6.07	31.0	720.0	432
107	Kampani	0.170111	7.150001	7 mpmoone	110	7.2	0.07	51.0	720.0	132
ZNG	Kodon Bosso	6.255	9.675833	Amphibolite/ Sch	189	10.2	6.83	30.0	29.8	169.4
108										
ZNG	Kaliko	6.204722	9.730278	Amp/Granite	163	5.5	7.26	31.3	244.0	149.6
109 ZNG	Makusidi	6.482778	9.6775	S/Stone	276	9.1	7.47	29.8	165.0	966
2NG 110	Iviakusiui	0.462776	9.0773	S/Stolle	270	9.1	/. 4 /	29.0	105.0	900
ZNG	Gudugi	6.050278	9.719444	S/Stone	96	10.7	6.44	28.7	238.0	141.7
111	C									
ZNG	Toroko	6.028333	9.5025	S/Stone	131	11.0	6.52	30.4	136.1	81.1
112	. ·	C 0.4 C 2.00	0.565000	G/G,	120	10.2	6.76	20.0	100 0	256
ZNG 113	Tangwagi	6.046389	9.567222	S/Stone	139	10.3	6.76	28.9	423.0	256
ZNG	Zungeru	6.151111	9.788611	Amph/Granite/Schis	125	6.1	6.98	29.0	452.0	272
114	Zungoru	0.101111	7.700011	t	123	0.1	0.70	<i>_</i> ,	152.0	<i>- 1 -</i>
ZNG	Laga	6.077222	9.531667	S/Stone	152	12.3	6.94	29.7	301	179.3
115										

ZNG	Kodo	6.115833	9.605833	S/Stone	114	8.3	6.18	35.1	108.5	65.1
116										
ZNG	Dabiri	6.031944	9.618056	S/Stone	91	8.7	7.07	38.0	375	229
117 ZNG	V1	6 1025	0.626529	0/04	118	11.2	6.62	40.7	256	152.5
2NG 118	Kanko	6.1025	9.636528	S/Stone	118	11.2	6.63	40.7	256	153.5
ZNG	Epigi	6.415556	9.5825	Granite	285	4.5	6.79	40.0	227	127.3
119	25.8.	0	y.e 02e	Claime	200		0.75	1010	,	127.5
ZNG	Kunu	6.418333	9.971111	Granite	227	5.1	6.51	18.9	402	241
120										
ZNG	Yakila	6.138056	9.947778	Schist/Granite	231	3.9	7.04	20.6	596	287
121 ZNG	Garin Gabas	6.118611	9.912778	schist/Granite	224	5.3	6.56	27.3	812	487
2NG 122	Garin Gabas	0.118011	9.912778	schist/Granite	224	3.3	0.30	21.3	812	46/
ZNG	KPAKARA	6.004167	9.789167	Granite/GNEISS	192	7.9	6.55	24.0	118.5	71.1
123										
ZNG	Katako	6.158056	9.983889	GRANITE/Schist	276	4.8	6.77	37.7	480	288
124										
ZNG	USHAMA	6.045	9.877222	Schist /Granite	201	5.6	7.14	36.3	572	344
125 ZNG	Gulenge	6.006111	9.991944	Schist/Granite	182	4.6	7.28	36.0	493	296
126	Gulenge	0.000111	7.7717 44	Schist/Granite	162	4.0	7.20	30.0	433	290
ZNG	Pangu	6.311389	9.989167	schist/Granite	398	6.0	7.78	35.7	153.6	92
127	\mathcal{E}									
ZNG	Rugan Alh	6.273333	9.908611	schist/Granite	153	4.8	7.17	23.5	233	139.9
128	Ahmadu									
ZNG	Wushishi	6.079889	9.728667	S/Stone	130	12.1	7.05	26.9	372	222.2
129 ZNG13	Iongoru	6.060833	9.820278	Granite	130	4.6	7.06	28.0	114.5	687
2NG13 0	Jangaru	0.000033	7.0202/8	Granite	130	4.0	7.00	∠0.U	114.3	00/
ZNG13	Gungu	6.312222	9.905833	Amphibolite/Sch/gr	178	3.9	5.25	32.8	89.9	51.3
1	<i>-</i>			anite						

ZNG13	Beri	6.493611	9.915278	Granitic Gneiss	213	4.7	5.58	36.1	58.8	34.4
2 ZNG13	Manta	6.436667	9.868889	Granitic Gneiss	223	2.8	6.98	35.6	119.6	717
3 ZNG13	Maikakaki	6.389444	9.881389	Granite	177	3.6	6.7	37.2	241	144.5
4 ZNG13	Daga Tshoho	6.499444	9.898333	Granite	199	4.4	6.62	33.6	284	169.2
5 ZNG13	pai	6.204722	9.583889	S/Stone & Schist	178	7.2	7.43	30.7	410	246
6 ZNG13	Takunpata	6.194722	9.553889	S/stone	156	8.9	6.55	36.5	126.5	76
7 ZNG13	(Makera) Evuntagi	6.144167	9.515833	S/stone	178	7.7	6.66	33.8	102.0	612
8 ZNG13	Malagi	6.104444	9.541944	S/Stone	141	9.2	6.62	37.0	271	162.6
9 ZNG14	Dukunsakun	6.036111	9.583889	S/Stone	101	10.3	6.67	38.0	284	169.7
0 ZNG14	Maito	6.028333	9.657778	S/Stone	92	4.0	5.88	37.9	30,2	18.01
1 ZNG14	Kutunku	6.061389	9.781111	Granite	114	3.9	6.45	38.7	798	477
2 ZNG	Dankuwagi	6.103611	9.644722	S/Stone	124	11.2	4.8	40.1	626	378
143 ZNG14	Kamfanin kirya	6.176111	9.756667	Granite/	142	7.0	5.22	35.2	19.6	11.71
4 ZNG	Gidan Gwari	6.109306	9.723333	Amphibolite S/Stone	144	5.0	6.97	33.4	186.2	112
145	Glam Gwarf	0.10/500).12333	S, Stone	111	<i>5.</i> 0	0.71	55.1	100.2	112

The Schoeller plot was used to show the distribution and concentrations of the major ions in the groundwater, the Ca ion dominating the cations while HCO₃ predominate the major anions. However,

there are seasonal variations of these ions as illustrated by figures below.

Schoeller diagram of the major ion's concentration in groundwater for season one

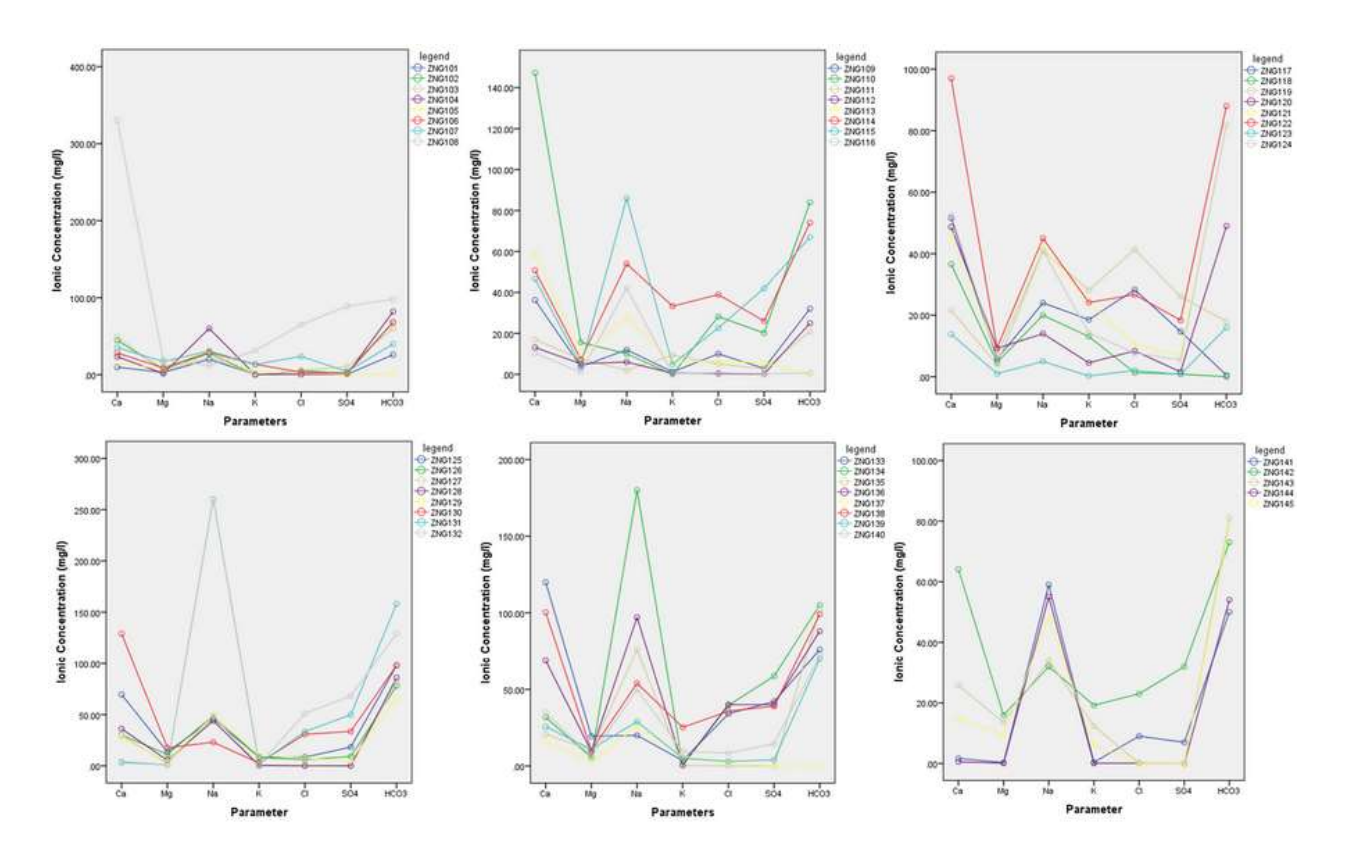


Figure 3: Schoeller Plot of the study area

pН

This represents the concentration of hydrogen ion in water and is the acidic property of water. The acids and free carbon dioxide lower water pH while carbonates, bicarbonates, hydroxides, phosphates, and silicates tend to raise water pH. Recorded water pH of sampled water range between 4.8 and 7.78 with an average of 6.3. All the pH values were within the MPL range of the 6.5 and 8.5. The pH of water determines to some extent the hydro geochemical reactions of groundwater within the

geological Formations that stores and releases groundwater.

Total Dissolved Solids (TDS)

This is an approximation of the total amount of mineral matter constituents of water, primarily these includes Ca, Cl, K, Mg, Na, NO₃, bicarbonates ions. TDS had a range of 11.71 – 966 mg/L with a recorded mean value of 225.67 mg/L. Only three (ZNG130, ZNG138 and ZNG 110) out of the total water samples analyzed had their TDS values above the MPL value of 500 mg/L of both the NSDWQ and WHO.

Electrical Conductivity (EC)

The Conductivity of water is the indicator of the salinity or the mineral content of water. Electrical conductivity measures the ability of water to conduct an electrical current. The higher the concentration of dissolved charged chemicals (also known as salts) in the water, the greater the electrical current that can be conducted. Charged anions and cations that naturally occur in water like Ca²⁺, Mg²⁺, K⁺, Cl⁻, SO₄⁺² and NO₄⁻ are responsible for the carrying electric current in solution, The higher the temperature of the water, the greater the ability of the water to conduct charge. Measured EC electrical groundwater in the area of study is between 19.6 and 812 µS/cm with an average of 446.4 µS/cm. None of the samples had EC values above the MPL of 1000 µS/cm.

Discussion of Results of Physical Parameters

The result revealed that among the cations detected in the sampled groundwater in the area revealed that Ca2+ ions dominate the other metals in the water with the order of given as Ca>Mg>Na>K. dominance However, the concentration of anions in the groundwater showed that Bicarbonate dominates the other non- metals in groundwater in the following order HCO₃⁻ > $NO_3 >$ $SO_4^2 > F - > PO_4^-$. dominance of calcium and bicarbonate in the groundwater can be related to the geology of the area while the presence of high concentration of NO₃⁻ and Cl⁻ in some locations can be related to anthropogenic sources rather than geology through poor waste disposal or Agricultural practices like application on farms. The groundwater in the area is weakly acidic based on the average PH value of 6.32. The Total dissolved solids (TDS) in groundwater of the area had an average value of 230.9 mg/L and the classification of Carroll (1962) Table 5 revealed the water to be fresh water of low dissolved chemical constituents.

Table 5: Classification of saline groundwater (After Carroll 1962)

Name or category of Water	Concentration of TDS (mg/L)
Fresh Water	0 -1,000
Brackish Water	1,000 - 10,000
Saline Water	10,000 - 100,000
Brine Water	>100, 000

Groundwater Chemical Characterization and Evolution

Groundwater Facies (types) of the Study Area

The hydrogeochemical data were subjected to different analyses and evaluations in order to determine the different water types in the area based on the chemical composition. Different Graphical presentations that include the Piper trilinear plot, the Durov plot, the Schoeller and the Stiff plots were employed to categorize the groundwater from the study area.

The Piper Plots

According to Piper (1944), the geochemical evolution of ground water can understood by plotting the concentrations of major cations and anions on a trilinear diagram (Piper). The position of an analysis that is plotted on a Piper diagram can be used to make a tentative conclusion as to the origin of the water represented by the analysis. Four basic conclusions can be derived from the multiple analyses plotted on Piper diagrams. These are water types, precipitation, or solution, mixing and ion exchange. Piper diagram divides water into four basic types according to their placement near the four corners of the diamonds. Water that plots at the top of diamond is high in Ca2+ + Mg2+ and Cl- + SO4 2-; which results in an area of permanent hardness. The water that plots near left corner is rich in Ca2+ + Mg2+ and HCO3 - and is the region of water of temporary hardness. Water plotted at the lower corner of the diamond is primarily composed of alkali carbonates (Na+ + K+ and HCO3 - + CO3 -), water lying near the right-hand side of the diamond may be considered saline (Na++K+ and Cl-+SO4 2-).

The Piper plot was used to demarcate the different water facies in the study area for both the wet and dry season. According to figure 4a, the Wet season is dominated by two types of water, the Ca-Cl type and the Mixed Ca-Cl-SO₄ type, these occupied fields 2 and 5 in the central diamond shape. The Ca-Cl constitutes more than 97 % of the water type in the study area while the Mixed Ca-Cl-SO₄ type occurred in only one (ZNG112) out of the 45 samples analyzed. The Ca-Cl facies is mainly associated with ion exchange hydro geochemical processes occurring in the sub-surface between the different cations in aguifer and the groundwater. The Ca-Cl water type is water of secondary salinity and of non-carbonate hardness with the strong acid dominating the weak acid in water. The dry season contain different water type which are shown in the figur8b, these are the Ca-HCO₃ Type, Ca-Cl type, Na-Cl type, Mixed Ca-Na-HCO₃ type, Mixed Ca-Cl-HCO₃ type, and the Na-HCO₃ type, which occupied fields 1, 2, 3, 4, 5 and 6 respectively on the diamond shape of the piper trilinear plot. The field 5 on the central diamond shaped plot represent the mixed water type Ca-Cl-HCO₃ which resulted from simple dissolution and mixing within the aquifer this dominate the other water types since it presents in 15 out of the total sampled water is equivalent to 33.3 % of the area. The Ca-Cl in shown to occupy field 2 on diamond plot with 13 out of the samples analyzed fallen into this facie taken up 28.9 % of the study area, the likely source of this water type is the ion exchange geochemical process through the rock-water interaction within the sub surface. The next dominant water specie is

the Na-Cl type which is water of primary salinity (Non-Carbonate Alkali) this water is in field 3 with 8 out of the total groundwater samples belong to this category which also represents 17.77 % of the area, this type of water type is associated with coastal areas with high salinity. Field 1 contains water secondary alkalinity and of carbonate hardness with alkali earth metals dominating while weak acid dominating strong acid. This water represent water from recharge areas which are also fresh and mostly water from area with carbonate rocks. Only four samples represented this water type in this study which constitute 8.88 % of the area of study. The sources of the water type can be due to

water-rock interaction and ion exchange process between aquifer and groundwater through weathering, dissolution, adsorption processes. The field number 6 contain the Na-HCO₃ water type which is water of primary alkalinity which are soft water. With only 2 of the samples water contain in this group which represents 4.44 % of the water from the area, this water type is form from ion exchange during which Na replaces Ca in the groundwater. The mixed water type Ca-Na-HCO₃ falls in field 4 of the plot and contain just 2 water samples 4.44 %, which also originate from dissolution and mixing processes in the subsurface.

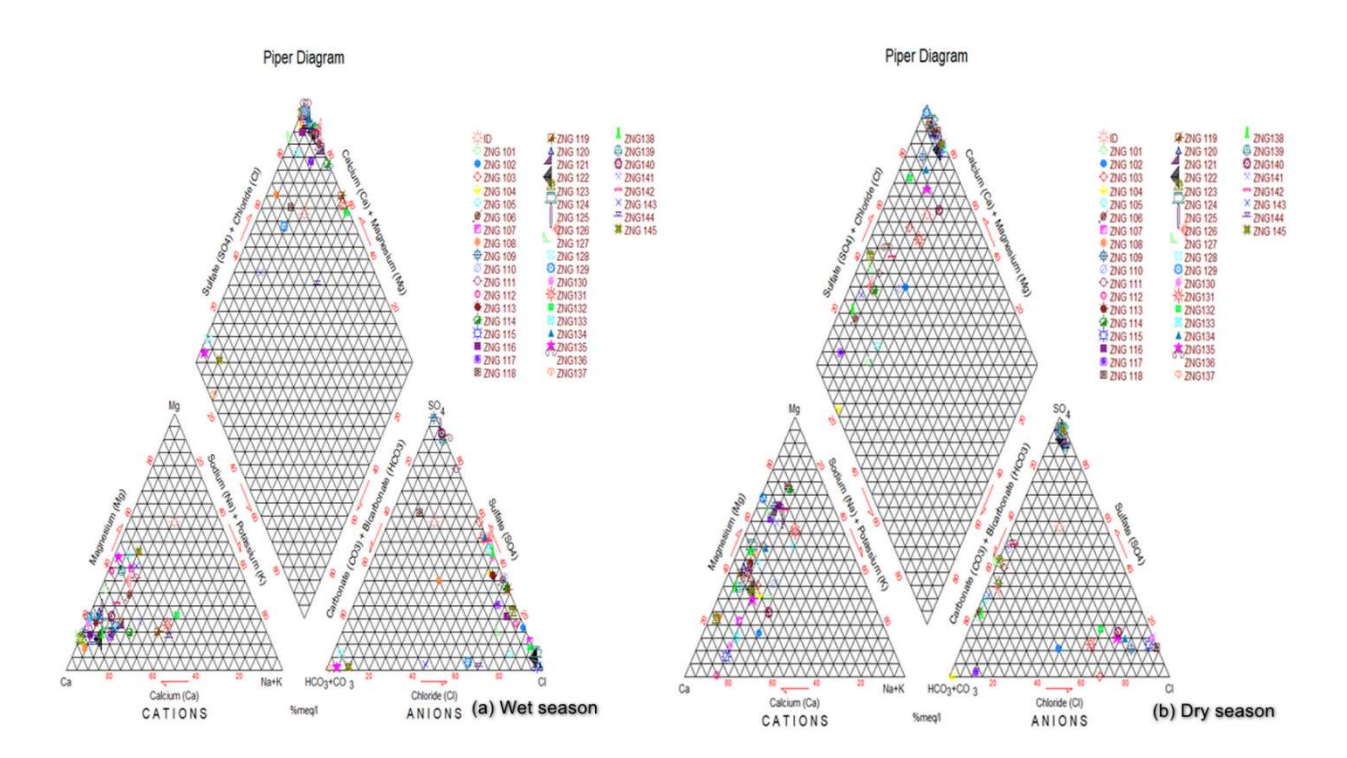


Figure 4: Piper plot for (a) wet season (b) dry season

The Durov Plot

Durov (1948) modified the piper trilinear diagram for the plotting of different water types and also for explaining the different hydro geochemical processes responsible for the presence of the different chemical parameters in groundwater. The Durov plots for both rainy and dry seasons (Figures 5a and 5b) were used to shed light on the hydro-geochemical processes in ground water aquifers in the study area. During the rainy season, the reverse ion exchange is responsible for the majority of ions in the groundwater this is seen in the field 1 and 4 in the diagram above. Ca-Cl is the dominant water type for the season with high concentration in field 1. Fields 2 and 3 represent ion exchange that led to the formation of the HCO₃ water, while field 5 in the projected rectangle represent mixed water that resulted from mixing and dissolution process with only Ca-Cl-HCO₃.

During the dry season (Figure 5b) the reverse ion exchange, forward ion

exchange and simple dissolution are the geochemical processes that operate to produce the different groundwater types in the area. Field 1 is the Ca-Cl type is predominate followed by field 6 with Mg-Cl, these are produced from ion exchange processes. The Ca-HCO₃, in field 3 and field 4 the Ca-Mg-HCO₃, are the product of reverse ion exchange where Na is been replaced by the Ca and Mg in the water. Field 5 contains the mixed water types were no particular anion or cations dominate this was possible through the simple dissolution and ion mixing processes.

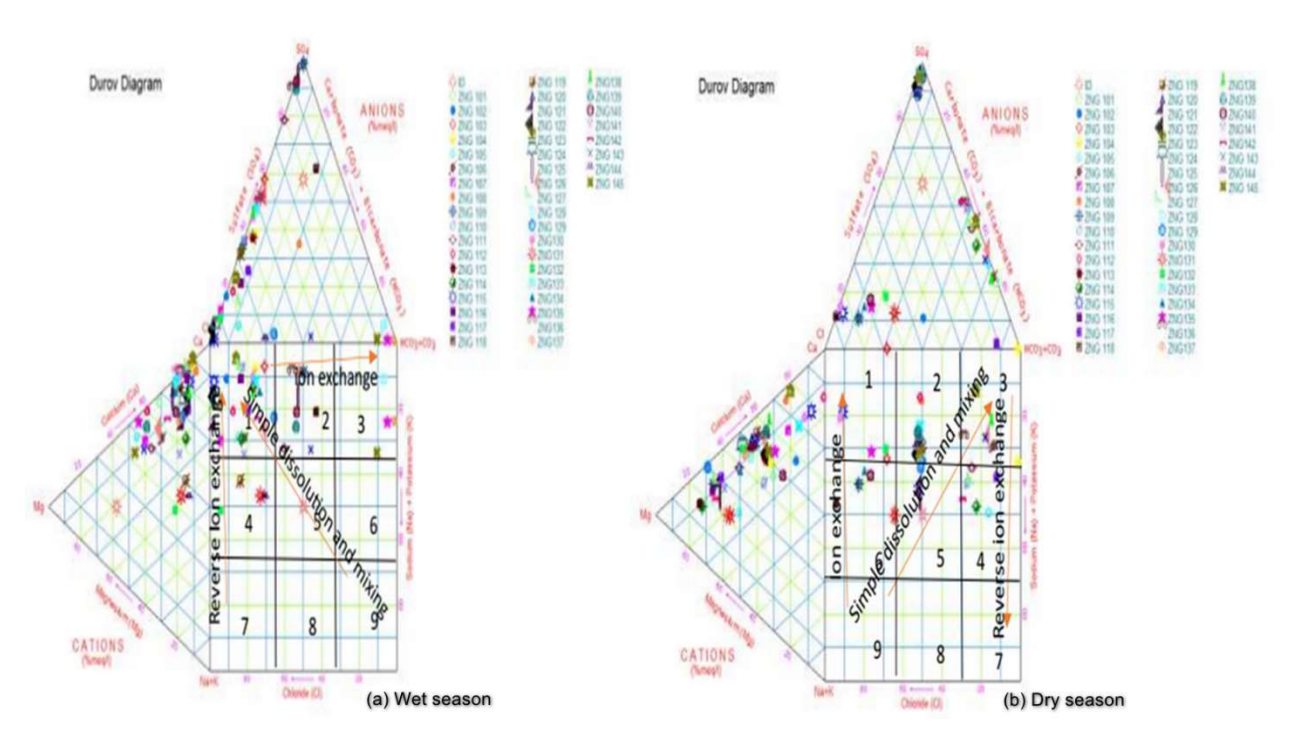


Figure 5: Durov plot for (a) wet season (b) dry season

Stiff Pattern Plots

Stiff diagrams, first suggested by Stiff (1951) for representing chemical analyses by four parallel horizontal and one vertical axes. Concentrations (meq/L) of four major cations (Na⁺, K⁺, Ca²⁺, Mg2⁺) are plotted to the left of a vertical zero axis and four major

anions (Cl–, SO4^{2–}, HCO3 ^{–,} NO3[–] + PO4 ^{2–}) to the right. The resulting points, when connected, form an irregular polygonal pattern; waters of a similar quality define a distinctive shape.

From the Stiff diagram plots (Figure 6) of the study area, the anion abundance relates and agrees well with the Piper diagram and Durov diagram by that the dominant anion is chloride followed by bicarbonates while the dominant cation is Calcium followed by Magnesium and sodium. This water has the same source and is from the same aquifer system.

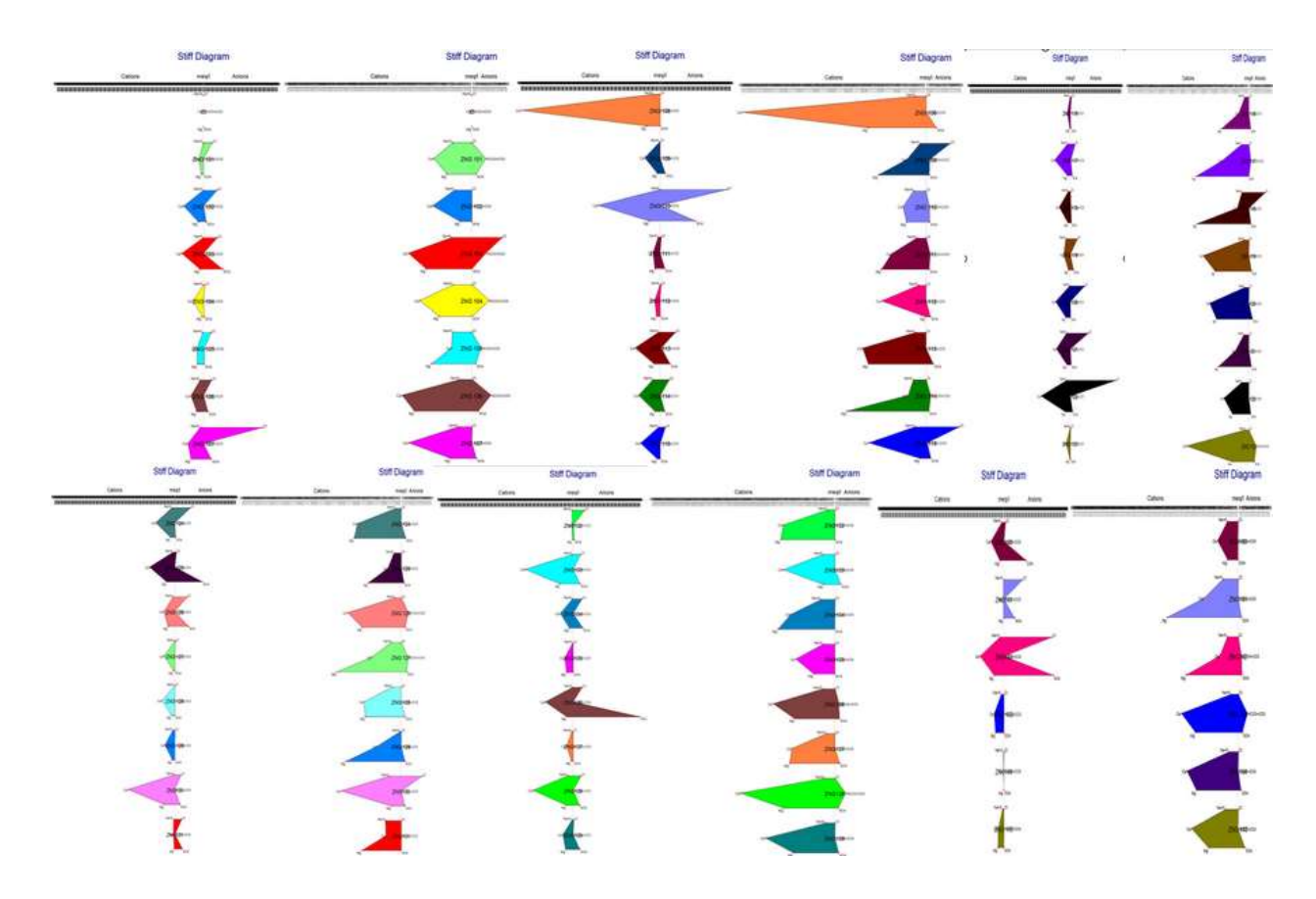


Figure 6: Stiff plots showing seasonal variations in water types in the study area

The Gibbs Plot

The Gibbs diagram is widely used to establish the relationship of composition and aquifer lithological characteristics (Gibbs, 1970). Three distinct fields such as precipitation dominance, evaporation dominance and rock water interaction dominance areas are shown in the Gibbs diagram (Figure 7a & 7b). The plot was obtained by plotting the measured TDS values of groundwater for both wet and dry seasons against the ratios of Na/ (Na + Ca) and Cl/ (Cl +HCO₃) for both cations and anions in groundwater, respectively. Based on figures 10a &10b for the rainy season 33 out of the total sampled groundwater which represent 73.3 % of the samples falls within the Rock- weathering domain of the Gibbs diagram, this was followed precipitation domain with 11 samples representing 24.4 % of the samples analyzed. The evaporation domain contains only one sample out of the total sample.

This revealed that majority of both the Cations and Anions of groundwater were derived from the rock-water interaction through weathering, dissolution and ion exchange processes between the aquifer and groundwater. However, for those samples that falls within the precipitation domain, these were added through rainfall which infiltrated into the groundwater body.

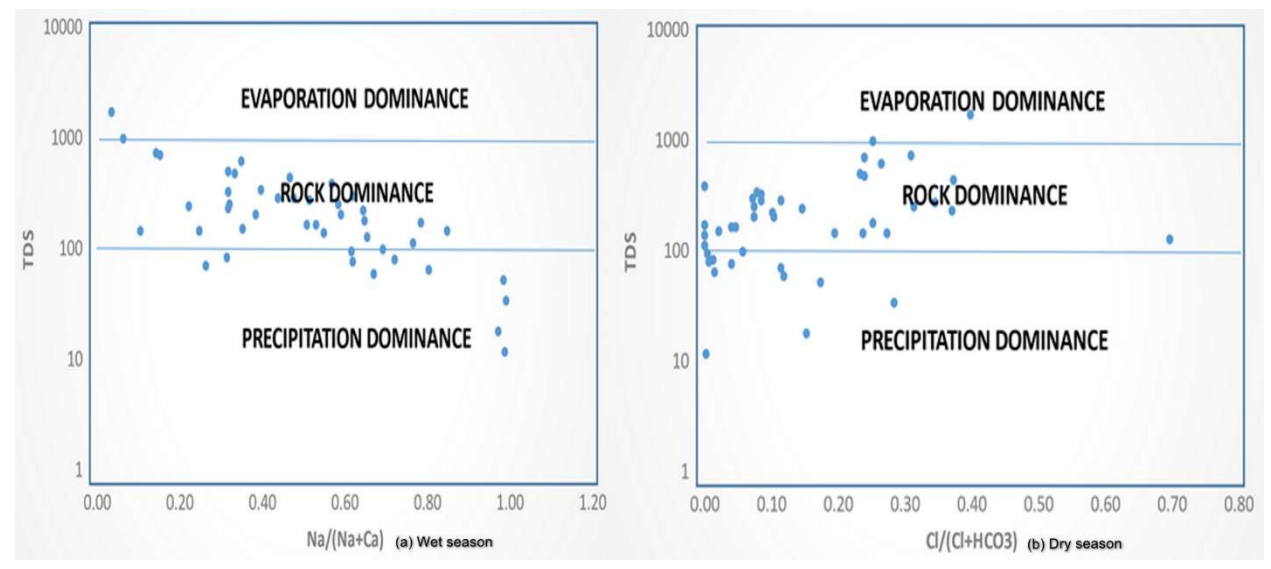


Figure 7: Gibbs diagram for (a) wet season and (b) dry season

CONCLUSION

Hydrochemical analysis conducted in the study area provides valuable insights into the sources and characteristics of major ions in groundwater. The concentration ranges and average values of various ions, including calcium, magnesium, sodium, potassium, bicarbonate, sulphate, chloride, nitrate. fluoride. phosphate, and determined. ammonium. were and compared against the Nigerian standard for drinking water quality (NSDWQ) and the Organization World Health (WHO) acceptable limits. Overall, the concentrations of these ions generally fell within the permissible limits set by both regulatory bodies, indicating that the groundwater in the study area is suitable for drinking purposes.

Calcium (Ca2+) and bicarbonate (HCO3-) were found to be the dominant cation and anion, respectively, in the groundwater, which can be attributed to the geological characteristics of the area. The presence of calcium may be attributed to the dissolution of calcium-rich rocks, while bicarbonate dominance suggests the influence of carbonate rocks on groundwater composition.

The analysis of physical parameters such as pH, total dissolved solids (TDS), and electrical conductivity (EC) further characterized the groundwater quality. The pH values ranged from acidic to slightly alkaline, with all values falling within the acceptable range for drinking water. Similarly, TDS and EC values were within permissible limits, indicating low levels of dissolved mineral constituents in the groundwater.

The groundwater facies analysis using Piper plots revealed distinct water types in both wet and dry seasons, with variations attributed hydrological to seasonal processes and geochemical interactions. The dominance of calcium-chloride (Ca-Cl) water type suggests ion exchange processes occurring within the aquifer system. Durov plots provided insights into hydrogeochemical processes influencing groundwater composition, including reverse ion exchange, forward ion exchange, and simple dissolution. The Stiff diagrams corroborated the findings from Piper and Durov plots, highlighting the dominance of chloride and bicarbonate ions in groundwater. Gibbs diagram illustrated the relationship between water composition and aquifer lithological characteristics, with the majority of groundwater samples indicating rock-water interaction as the primary source of ions.

The comprehensive hydrochemical analysis conducted in the study area enhances our understanding of groundwater quality, sources of major ions, and hydrogeochemical processes influencing groundwater evolution. The findings provide valuable information for water resource management and environmental conservation efforts in the region. Further research and monitoring are recommended to assess long-term trends and potential anthropogenic impacts on groundwater quality.

REFERENCES

Acharya, G., & Barbier, E. B. (2000). Valuing groundwater recharge through agricultural production in the Hadejia-Nguru wetlands in

- northern Nigeria. *Agricultural Economics*, *22*(3), 247–259. https://doi.org/10.1111/j.1574-0862.2000.tb00073.x
- Adimalla, N., & Venkatayogi, S. (2018).

 Geochemical characterization and evaluation of groundwater suitability for domestic and agricultural utility in the semi-arid region of Basara, Telangana State, South India. *Appl. Water Sci.* 8 (1).
- Agbor, A. T. (2014). Geology and geochemistry of Zungeru amphibolites, north Central Nigeria. Universal Journal of Geoscience, 2(4), 116-122.
- Ahmad, A., Mohammad, A. A., Majeda, K., & Nabil, Z. (2020). Hydrogeochemical characterization and quality evaluation of groundwater suitability for domestic and agricultural uses in the state of Qatar. Groundwater for Sustainable Development 11.
- Ajibade, A. C. (1980). Geotectonic evolution of the Zungeru region, Nigeria (Doctoral dissertation, University College of Wales).
- Ajibade, A. C., Fitches, W. R., & Wright, J. B. (1979). The Zungeru mylonites, Nigeria: recognition of a major tectonic unit. Revue de géologie dynamique et de géographie physique Paris, 21(5), 359-363.
- Akakuru, O.C., & Akudinobi, B.E.B (2018).

 Determination of water quality index and irrigation suitability of groundwater sources in parts of coastal aquifers of Eastern Niger

- Delta, Nigeria. *International Journal of Applied and Natural Sciences (IJANS)*, 7 (1): 1-6. www.iaset.us
- Akakuru, O.C., Akudinobi, B.E., Nwankwoala, H.O. *et al* (2021). Compendious evaluation of groundwater in parts of Asaba, Nigeria for agricultural sustainability. *Geosci J* https://doi.org/10.1007/s12303-021-0010-x
- Akakuru, O.C., Akudinobi, B.E.B, & Usman, A.O (2017). Organic and heavy metal assessment of groundwater sources around Nigeria National Petroleum Corporation oil depot Aba, Southeastern Nigeria. *Journal of Natural Sciences Research*, 7(24): 48-58.
- Akakuru, O.C., Maduka, E.C, & Akakuru, O.U (2013). Hydrogeochemical characterization of surface water sources in Owerri Capital Territory, Southeastern Nigeria, *IOSR Journal of Applied Geology and Geophysics*, 1(2), www.iosrjournals.org.
- Akaolisa, C.C.Z., Agbasi, O., Okeke, O.C. and Okechukwu, S., (2022b) An assessment of the groundwater potentials of the farm with preliminary geophysical method and grain size analysis prior to the drilling of boreholes. *HydroResearch*, [online] 5, pp.85–98. Available at: http://dx.doi.org/10.1016/j.hydres.2 022.09.001.
- Akaolisa, C.C.Z., Ibeneche, W., Ibeneme, S., Agbasi, O. and Okechukwu, S.,

- (2022a)Enhance groundwater quality assessment using integrated vertical electrical sounding and physio-chemical analyses Umuahia South, Nigeria. International Journal of Energy and Water Resources. [online] Available at: http://dx.doi.org/10.1007/s42108-022-00219-8.
- Akinfemiwa Akanbi, O., & Kofoworola Akinseye, E. (2023). Assessment of nitrate, trace elements and bacterial contamination of groundwater in ilora area of southwestern Nigeria. *Global Journal of Pure and Applied Sciences*, 29(1), 105–112. https://doi.org/10.4314/gjpas.v29i1.13
- APHA (1998). Standard Methods for Examination of Water and Wastewater. Washington, D.C
 - Dewey, J. F., & Burke, K. C. (1973). Tibetan, Variscan, and Precambrian basement reactivation: products of continental collision. The Journal of Geology, 81(6), 683-692.
- Egbueri, J. C. (2019). Evaluation and characterization of the groundwater quality and hydrogeochemistry of Ogbaru farming district in southeastern Nigeria. *SN Applied Sciences*, 1:851
- Egbuniwe, I. G., Fitches, W. R., Bentley, M., & Snelling, N. J. (1985). Late Pan-African syenite-granite plutons in NW Nigeria. Journal of African earth sciences (1983), 3(4), 427-435.

- Ejiogu, B. C., Opara, A. I, Nwosu, E. I., Nwofor, O. K., Onyema, J. C., & Chinaka, J. C. (2019). Estimates of geohydraulic aquifer vulnerability characteristics of Imo State and environs, Southeastern electrical Nigeria, using conductivity data. Environmental Monitoring and Assessment 191(4):238. (Springer), DOI: 10.1007/s10661-019-7335-1
- Elango, L., & Kannan, R. (2007). Rock—water interaction and its control on chemical composition of groundwater. Developments in environmental science, 5, 229-243.
- Eyankware, M.O, P.N Obasi, O.O Omo-Irabor, O.C Akakuru (2020). Hydrochemical characterization of an abandoned quarry and mine water for domestic and irrigation uses in Abakaliki, southeast Nigeria. *Model. Earth Syst. Environ.* (2020). https://doi.org/10.1007/s40808-020-00827-5
- Golchin, I., & Azhdary Moghaddam, M. (2016). Hydro-geochemical characteristics and groundwater quality assessment in Iranshahr plain aquifer, Iran. Environmental Earth Sciences, 75, 1-14.
- Gopinath, S, K., Srinivasamoorthy, K., Saravanan, R., Prakash & D. Karunanidhi (2019): Characterizing groundwater quality and seawater intrusion in coastal aquifers of Nagapattinam and Karaikal, South India using hydrogeochemistry and modelling techniques, *Human and*

- Ecological Risk Assessment: An International Journal. 1-22.
- He, X., Wu, J., & He, S. (2019).

 Hydrochemical characteristics and quality evaluation of groundwater in terms of health risks in Luohe aquifer in Wuqi County of the Chinese Loess Plateau, northwest China. *Human and Ecological Risk Assessment*, 25(1–2), 32–51. DOI: 10.1080/10807039.2018.1531693
- Hussaini, A., & Matazu, B. M. (2023). An overview of key improvements by the Nigerian Meteorological Agency for the modernisation of meteorological services in Nigeria. Science World Journal, 18(1), 152-157.
- Ibe, F.C., Opara, A.I., & Ibe, B.O (2020). Application of pollution evaluation models in groundwater the vicinity of systems in automobile scrap markets in Owerri municipal and environs, southeastern Nigeria; Scientific (Elsevier), African 8, e00450(Online First). DOI: 10.1016/j.sciaf.2020.e00450.
- Ige, O. O., Adewoye, F. O., & Obasaju, D. O. (2021). Hydrochemical evaluation of groundwater quality: a case study from parts of North-Central, Nigeria. *Sustainable Water Resources Management*, 7(6). https://doi.org/10.1007/s40899-021-00577-x
- Klemm, D. D., Schneider, W., & Wagner, B. (1984). The Precambrian metavolcano-sedimentary sequence east of Ife and Ilesha/SW Nigeria. A

- Nigerian 'greenstone belt'. Journal of African Earth Sciences (1983), 2(2), 161-176.
- Lawal, A., Tijani, M. N., Snow, D., & D'Alessio, M. (2022). Quality and hydrochemical assessment groundwater in geological transition zones: a case study from Nigeria. N.E. Environmental Science and Pollution Research, 10643-10663. 30(4),https://doi.org/10.1007/s11356-022-22762-x
- Long, Y., Huang, T., Zhang, F., Li, Z., Ma, B., Li, Y., & Pang, Z. (2021). Origin of sulphate in the unsaturated zone and groundwater of a loess aquifer. *Hydrological Processes*, 35(4). https://doi.org/10.1002/hyp.14166
- McCurry, D. M. (1976). Cross-cultural models for Muslim evangelism. Missiology, 4(3), 267-283.
- Mokoena Portia, Thokozani Kanyerere, Jan van Bever Donker (2020). Hydrogeochemical characteristics and evaluation of groundwater quality for domestic and irrigation purposes: a case study of the Heuningnes Catchment, Western Cape Province, South Africa. SN Applied Sciences, 2:1548.
- Moussa, A. B., Sawsan, C., Houcem, M., Sarra, B. H., Salem, H. E., Kamel, Z., Amor, H., & Habib, M. (2020). Hydrogeochemistry and evaluation of groundwater suitability for irrigation purpose in the Mornag region, northeastern Tunisia. *Environment, Development and Sustainability.1-21*

- Ogezi, A. E. O. (1977). Geochemistry and geochronology of basement rocks from northwestern Nigeria (Doctoral dissertation, University of Leeds (Department of Earth Sciences)).
- Olade, M. A., & Elueze, A. A. (1979).

 Petrochemistry of the Ilesha amphibolites and Precambrian crustal evolution in the Pan-African domain of SW Nigeria.

 Precambrian Research, 8(3-4), 303-318.
- Onipe, T., Edokpayi, J. N., & Odiyo, J. O. (2020). A review on the potential sources and health implications of fluoride in groundwater of Sub-Saharan Africa. *Journal of Environmental Science and Health, Part A*, 55(9), 1078–1093. https://doi.org/10.1080/10934529.2 020.1770516
- Onyeanuna, C. Chukwuemeka, Patience John and N. Temple Nwankwo (2019). Geochemical characterization and assessment of groundwater quality in Owerri metropolis, South-Eastern Nigeria.

 Journal of Geography,
 Environment and Earth Science
 International, 19(1), 1-24.
- Oyawoye, M. O. (1972). The basement complex of Nigeria. African geology, 67-99.
- Piper, A. M. (1944). A graphic procedure in the geochemical interpretation of water analysis, *American Geophysical Union Transactions*, 25: 914-923.

- Rahaman, M. A. (1976). Review of the basement geology of south-western Nigeria.
- Raju, N.J., Shukla, U.K., & Ram, P. (2011). Hydrogeochemistry for the assessment of groundwater quality in Varanasi: a fast-urbanizing centre in Uttar Pradesh, India. *Environ Monit Assess* 173:279–300
- Saha, S, Selim, R., & Mrinal, K. R. (2019). Hydrochemical evaluation of groundwater quality of the Tista floodplain, Rangpur, Bangladesh. *Applied Water Science*, 9:198
- Sakram, G., & Adimalla, N. (2018).

 Hydrogeochemical characterization and assessment of water suitability for drinking and irrigation in crystalline rocks of Mothkur region, Telangana State, South India. *Appl Water Sci* 8, 143.

 https://doi.org/10.1007/s13201-018-0787-6
- Sakram, G., Sundaraiah, R., & Vishnu Bhoopathi, P. R. S. (2013). The impact of agricultural activity on the chemical quality of groundwater, Karanja Vagu Watershed, Medak District, Andhra Pradesh. *Int J Adv Sci Tech Res*, 6(3), 769-786.
- Sia Su G.L. (2008). Assessing the effect of a dumpsite to groundwater quality in Payatas, Phillipines. *American Journal of Environmental Sciences*, 4(4),276-280
- Sikakwe, G. U., & Eyong, G. A. (2022). Groundwater flow and geochemical processes affecting its quality in the

- basement (Oban Massif) and sedimentary (Mamfe Embayment) environments, southeastern Nigeria. *Journal of African Earth Sciences*, 188, 104467. https://doi.org/10.1016/j.jafrearsci. 2022.104467
- Siloko, O. G., Mojeed, M. A., & Alabi, R. O. (2022). Hydrochemical Properties and Groundwater Quality Assessment in Kurudu Area, Abuja, North Central Nigeria. *International Journal of Scientific and Research Publications*, *12*(11), 332–343. https://doi.org/10.29322/ijsrp.12.11.2022.p13142
- Stiff, H. A. Jr. (1951). The Interpretation of Chemical Water Analysis by means of Patterns. *Journal of Petroleum Technology* 3(10): 15-17
- Tiwari, A. K., Raffaella, G. M., & Muriel, L. (2017). Evaluation of hydrogeochemical processes and groundwater quality for suitability of drinking and irrigation purposes: a case study in the Aosta Valley region, Italy. *Arab J Geosci* (2017) 10:264 Todd DK, Ways LW (2004) Groundwater hydrology. Wiley, USA
- Todd, D. K. (1980). Groundwater hydrology, 2nd eds. *Wiley, New York*.
- Truswell, J. F., & Cope, R. N. (1963). The Geology of Parts of Niger and Zaria Provinces, Northern Nigeria: Explanation of 1: 250,000 Sheet No. 31. Federal Government of Nigeria.

- Turner, D. C. (1983). Upper Proterozoic schist belts in the Nigerian sector of the Pan-African province of West Africa. Precambrian research, 21(1-2), 55-79.
- Udoh, E. J., & Etim, N. A. (2007). Analysis of domestic water consumption pattern by farming households in Itu, Akwa Ibom State, Nigeria. *European Journal of Social Sciences*, 5(2), 76–82.
- United State Geological Survey (USGS), (2012). http://www.usgs.gov, 08/06/2012 11:45AM.)
- Urom, O.O., Opara, A.I., Usen, O.S. *et al.* (2021). Electro-geohydraulic estimation of shallow aquifers of Owerri and environs, Southeastern Nigeria using multiple empirical resistivity equations. *Int J Energy Water* Res. https://doi.org/10.1007/s42108-021-00122-8
- WHO (2017). Guidelines for drinking water quality. Stanford Geneva, Switzerland.
- Woakes, M., Rahaman, M. A., & Ajibade, A. C. (1987). Some metallogenetic features of the Nigerian basement.

- Journal of African Earth Sciences (1983), 6(5), 655-664.
- Wu, H., Dong, Y., Gao, L., Song, X., Liu, F., Peng, X., & Zhang, G. L. (2021). Identifying nitrate sources in surface water, regolith, and groundwater in a subtropical red soil Critical Zone by using dual nitrate isotopes. *CATENA*, *198*, 104994. https://doi.org/10.1016/j.catena.202 0.104994
- Wurtsbaugh, W. A., Paerl, H. W., & Dodds, W. K. (2019). Nutrients, eutrophication, and harmful algal blooms along the freshwater to marine continuum. *WIREs Water*, 6(5). https://doi.org/10.1002/wat2.1373
- Zacchaeus, O. O., Adeyemi, M. B., Azeem Adedeji, A., Adegoke, K. A., Anumah, A. O.,

Taiwo, A. M., & Ganiyu, S. A. (2020). Effects of industrialization on groundwater quality in Shagamu and Ota industrial areas of Ogun state, Nigeria. *Heliyon*, *6*(7), e04353.

https://doi.org/10.1016/j.heliyon.20 20.e04353